

# Engineering Notes

*ENGINEERING NOTES are short manuscripts describing new developments or important results of a preliminary nature. These Notes cannot exceed six manuscript pages and three figures; a page of text may be substituted for a figure and vice versa. After informal review by the editors, they may be published within a few months of the date of receipt. Style requirements are the same as for regular contributions (see inside back cover).*

## Solar-System Escape Trajectories Using Solar Sails

Deepti N. Sharma\* and D. J. Scheeres†

University of Michigan, Ann Arbor, Michigan 48109-2140

### I. Introduction

THE trajectory dynamics of a solar sail using a simple guidance strategy is studied to find zero-cost escape trajectories from the sun in minimal time spans. We specifically focus on finding the time to reach escape energy,  $\varepsilon = 0$ . We find that escape trajectories that first maximally decrease orbit energy and then maximally increase energy are generally more time efficient than escape trajectories that only maximally increase energy. Our simple guidance strategy compares well with optimized trajectories. Previous work on the topic of solar-system escape trajectories for solar sails has generally concentrated on high-energy trajectories designed for specific missions. Van der Ha and Modi<sup>1</sup> explored optimal solar-sail orientation for maximum increase in the total energy and angular momentum over one revolution of the spacecraft around the sun. Leipold and Wagner<sup>2</sup> investigated the generation of high orbital energies for solar sails using solar fly-bys. Sauer<sup>3</sup> has studied the optimization of solar-sail trajectories to minimize the time required to reach a certain solar distance. In contrast, our work examines the dynamics of solar-sail trajectories under simple guidance laws and focuses on their ability to escape from the solar system. An improved understanding of sail dynamics under simple guidance laws might aid in the development of sail trajectories and solar-sail missions.

We develop control laws for the angle of the solar sail with respect to the sun that optimize the rate of change of the semimajor axis, so that the spacecraft will decrease or increase energy at a maximal rate. Using this control law, we analyze several different escape trajectories, including escape from initially circular and elliptical orbits. We also study escape trajectories that start with the solar sail in a circular orbit at 1 astronomical unit (AU), spiral inward towards the sun by decreasing the energy of its orbit, and then, at a specified distance from the sun, switch to increasing orbit energy until escape. This trajectory allows the solar sail to gather energy from the increased solar radiation pressure near the sun and use it to achieve escape in a shorter time span. We have examined these trajectories in terms of their required solar-sail lightness number  $\beta$  and time for escape. We only consider solar sails with lightness numbers less than unity because a solar sail with a lightness number greater than one can achieve direct escape by orienting the sail full on to the sun.

Received 15 May 2003; revision received 21 January 2004; accepted for publication 16 February 2004. Copyright © 2004 by the American Institute of Aeronautics and Astronautics, Inc. All rights reserved. Copies of this paper may be made for personal or internal use, on condition that the copier pay the \$10.00 per-copy fee to the Copyright Clearance Center, Inc., 222 Rosewood Drive, Danvers, MA 01923; include the code 0022-4650/04 \$10.00 in correspondence with the CCC.

\*Graduate Student, Department of Aerospace Engineering; dsharma@umich.edu.

†Associate Professor, Department of Aerospace Engineering; scheeres@umich.edu. Associate Fellow AIAA.

For all cases escape is defined as the time at which orbital energy is equal to zero ( $\varepsilon = 0$ ) and does not preclude generation of additional energy increase.

From this study we have established that minimizing the time to escape does not necessarily involve maximizing the increase in orbit energy at every instant along the trajectory. We have also found that relatively poor performance solar sails can achieve an escape trajectory from the sun in less than one year.

### II. Locally Optimal Control Law

To simulate the orbital mechanics of a solar sail, we assume planar dynamics and an ideal solar sail, leading to the equations of motion in polar coordinates ( $r$ , radial position and  $\theta$ , angular position):

$$\ddot{r} = r\dot{\theta}^2 - \mu/r^2 + T_r \quad (1)$$

$$\ddot{\theta} = (T_\theta - 2\dot{r}\dot{\theta})/r \quad (2)$$

where  $T_r$  and  $T_\theta$  are the thrust vectors from the solar radiation pressure in the radial and transverse directions, respectively, and are defined by

$$T_r = \beta\mu \cos^3(\alpha)/r^2 \quad (3)$$

$$T_\theta = \beta\mu \cos^2(\alpha) \sin(\alpha)/r^2 \quad (4)$$

A local integration accuracy of  $3 \times 10^{-14}$  was used for the simulation of the equations of motion. The development of these relations and further discussion can be found in McInnes.<sup>4</sup> In these equations,  $\mu$  is the gravitational constant  $GM_{\text{Sun}}$  (normalized to 1) and  $\alpha$  is the angle between the sail normal and the sun line. If  $\alpha$  is 0, the sail is directed normal to the sun and can achieve maximum thrust (twice the momentum of incoming photons in a perfectly reflecting solar sail). The nondimensional solar-sail lightness number  $\beta$  is the ratio of the solar radiation pressure acceleration to the solar gravitational acceleration. At 1 AU, a  $\beta$  value of 1 corresponds to an acceleration of 5.93 mm/s<sup>2</sup>, equal to the local gravitational acceleration. The value of  $\beta$  is independent of the distance between the sun and the solar sail because both accelerations are assumed to have an inverse square relation. Solar sails with higher  $\beta$  values have greater acceleration and therefore better performance.

To find a guidance law for solar escape trajectories, we focused on manipulating  $\alpha$  (the angle between the sail normal and the sun line) so that the sail is always oriented to maximize or minimize the rate of orbital energy change. We used the following Gauss variational equation from McInnes<sup>4</sup> relating semimajor axis and true anomaly to maximize or minimize the rate of change in semimajor axis at every instant along its trajectory:

$$\frac{da}{df} = \frac{2pr^2}{\mu(1-e^2)^2} \left( T_r e \sin f + T_\theta \frac{p}{r} \right) \quad (5)$$

Here  $p = a(1-e^2)$ ,  $a = -\mu/2\varepsilon$  is the semimajor axis of the orbit,  $e = \sqrt{1+2\varepsilon h^2/\mu^2}$  is the eccentricity,  $\varepsilon = \frac{1}{2}(\dot{r}^2 + r^2\dot{\theta}^2) - \mu/r$  is the energy,  $h = r^2\dot{\theta}$  is the angular momentum, and  $T_r$  and  $T_\theta$  are the thrust vectors defined earlier. To find the value of  $\alpha$  that would maximally increase or decrease  $da/df$ , we took the partial derivative of  $da/df$  with respect to  $\alpha$ , set it equal to zero, and solved for  $\alpha$ :

$$\frac{\partial}{\partial \alpha} \frac{da}{df} = 0 \quad (6)$$

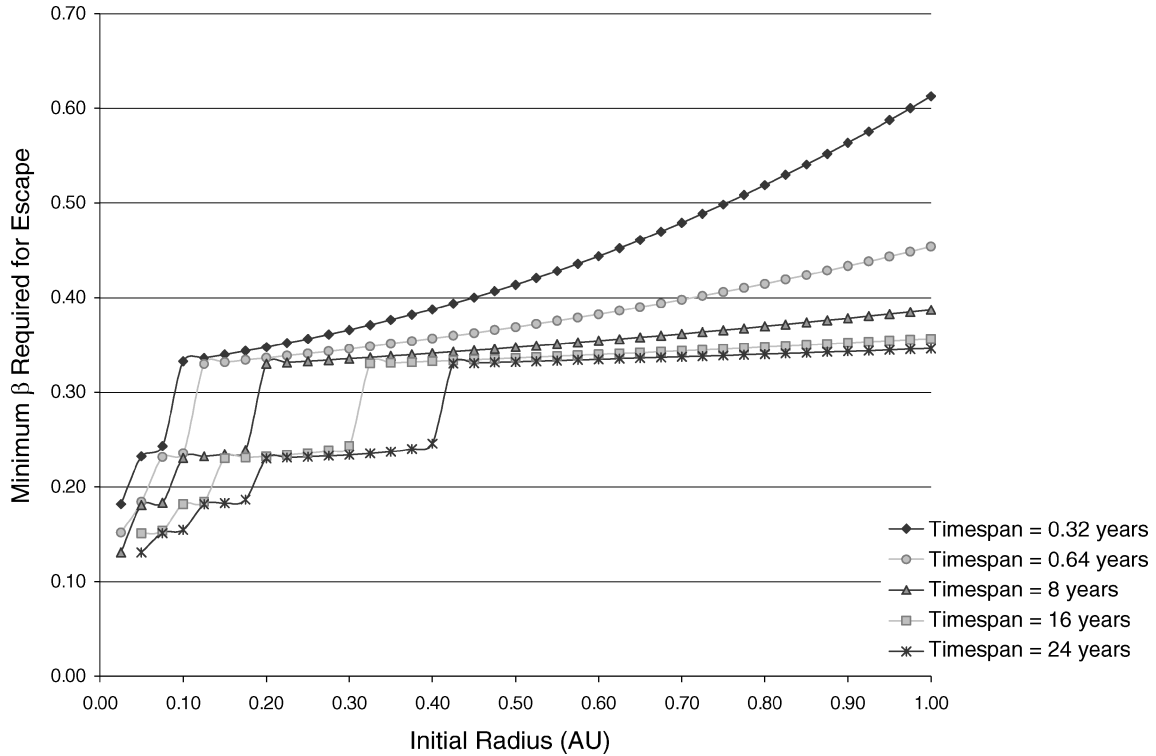


Fig. 1 Minimum  $\beta$  required for escape at a given radius, initially circular orbits.

The  $\alpha$  control law that maximally increases (+) or decreases (-) the semimajor axis is defined as

$$\alpha = \arctan\left(\frac{-3\dot{r}\sqrt{\mu}\sqrt{r^4\dot{\theta}^2/\mu} \pm \sqrt{9r^4\dot{\theta}^2\dot{r}^2 + 8r^6\dot{\theta}^4}}{4r^3\dot{\theta}^2}\right) \quad (7)$$

Using these controls for  $\alpha$ , we are able to maximally increase or decrease the semimajor axis and therefore the orbit energy at every instant in the trajectory. This locally optimal control can be used to study a variety of solar-sail escape trajectories.

### III. Escape Times with Maximizing Control

#### A. Initially Circular Orbits

We first examine the escape trajectories that result from applying the maximizing control law to initially circular trajectories, using the initial condition  $\dot{\theta} = \sqrt{(1/r^3)}$ , where  $r$  varies from 0 to 1 AU.

For this analysis, we set the initial radius of the orbit and determined the minimum value of the solar-sail lightness number  $\beta$  required for the solar sail to achieve escape in a given time span. Figure 1 shows the result of this analysis; the time spans in which the sail was to escape were set at 0.32, 0.64, 8, 16, and 24 years.

We see that for smaller radii a lower value of  $\beta$  is required for escape. As the sail gets closer to the sun, it gains more thrust from the increased solar radiation pressure and needs a less efficient sail to escape. We note that there is a large difference in the required  $\beta$  value for escape between shorter time spans (0.32 and 0.64 years), but for longer time spans the  $\beta$  value of the sail becomes less significant. It is apparent from Fig. 1 that there are discontinuous changes in  $\beta$  as the initial radius of the sail becomes small. These discontinuities occur in areas in which the sail becomes stranded in large elliptical orbits for a time before they escape. The curves step down to lower values of  $\beta$  as the trajectories start out closer to the sun, and the sail is no longer trapped in such an orbit.

#### B. Initially Eccentric Orbits

Escape trajectories resulting from application of the maximizing control law to initially eccentric orbits were also studied to understand the affect of eccentricity. We modeled these orbits using the

initial condition  $\dot{\theta} = \sqrt{[2r_p/(1+r_p)]}$  at  $r = 1$ , which corresponds to a variable initial radius of periapsis with the radius of apoapsis at 1 AU. We performed a similar analysis as before, varying the radius of periapsis of the orbit from 0 to 1 AU and determining the minimum value of  $\beta$  that would allow escape in time spans of 0.32, 0.64, 8, 16, and 24 years. The results of this analysis are shown in Fig. 2.

We see that for smaller radii of periapsis a lower value of  $\beta$  is required for the solar sail to escape because of the increased solar radiation pressure near the sun. But this relationship is not valid for larger radii of periapsis. For each time span, at a certain radius, as the radius of periapsis grows, the  $\beta$  values required for escape actually decrease. From Fig. 2, we see that for a sail with a  $\beta$  value above 0.6 at a 0.32-year escape time, 0.45 at 0.64 years, and 0.4 at 8–24 years, it is always best to begin escape from a circular orbit at 1 AU.

### IV. Escape Times with Minimizing/Maximizing Control

Wishing to capitalize on the best aspects of initially circular and elliptic escape trajectories, we analyzed a guidance approach in which the solar sail first spirals in toward the sun to take advantage of greater solar radiation pressure and increasing eccentricity, then spirals out to escape. In these escape trajectories the solar-sail spacecraft begins in a circular orbit at 1 AU (which corresponds to a low-energy escape from the Earth, perhaps using the solar sail) and uses the minimizing control law [Eq. (7) with the - sign] to decrease semimajor axis. At a specified distance from the sun, the control law is switched to maximally increase the orbit energy, so that the spacecraft increases its energy until it reaches escape. This trajectory allows the solar sail to take advantage of the increasing solar radiation pressure near the sun and use it to generate a faster time to escape.

We numerically simulated these minimizing/maximizing trajectories to obtain their total escape times. For a given  $\beta$ , we varied the distance at which the control law would be switched from minimizing orbit energy to maximizing orbit energy and found the resulting total escape times. The initial conditions used in this section all correspond to an initially circular orbit at 1 AU,  $r = 1$ ,  $\theta = 0$ ,  $\dot{r} = 0$ , and  $\dot{\theta} = 1$ .

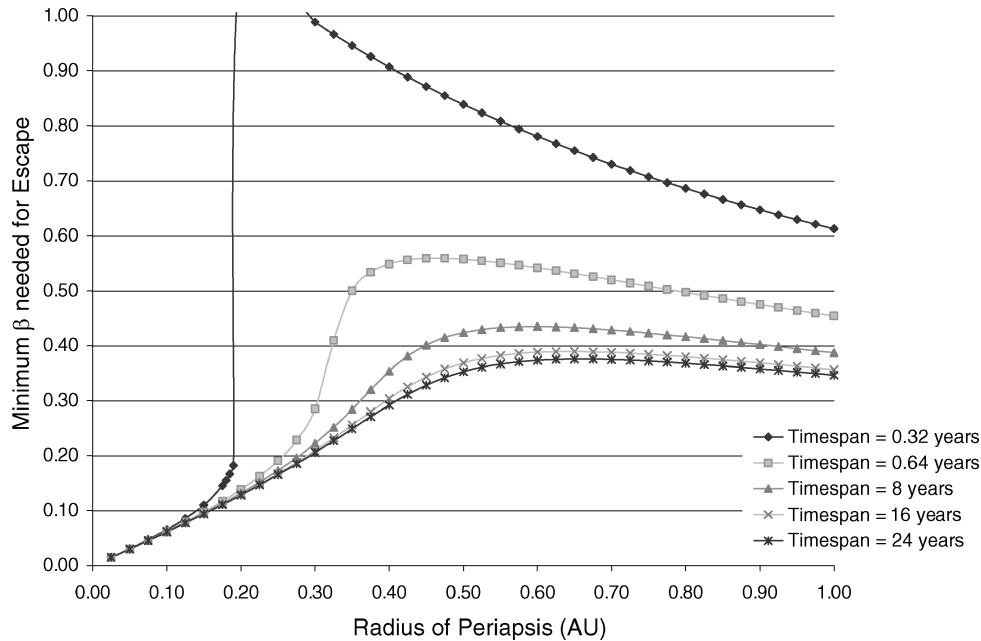


Fig. 2 Minimum  $\beta$  required for escape at a given radius of periapsis, initially eccentric orbits.

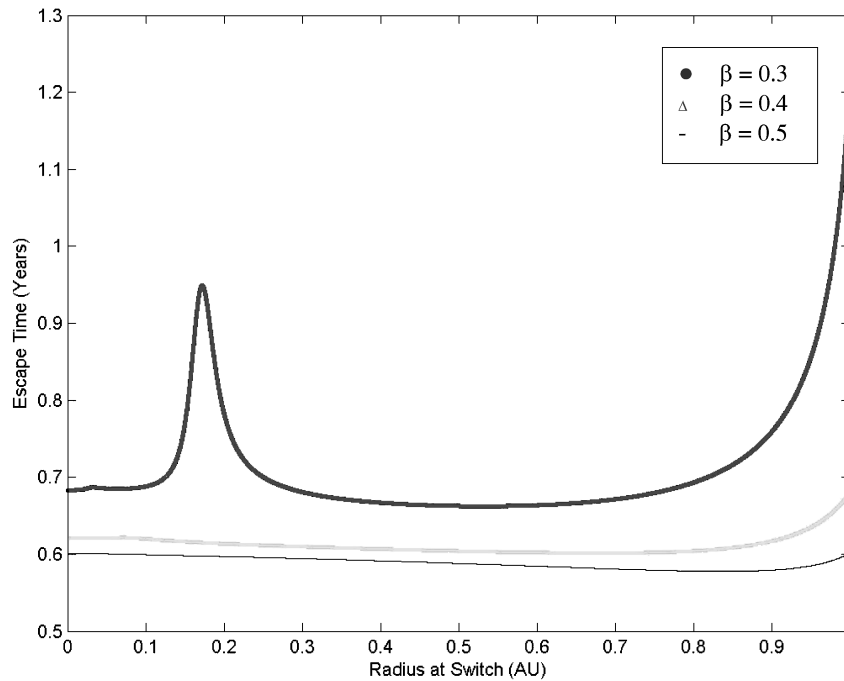


Fig. 3 Escape times at different switching distances.

The results of this analysis show that the variation of total escape time with switching distance can be highly dependent on  $\beta$ . From Fig. 3, in the plot of  $\beta = 0.3$ , it is apparent that the best times to switch controls are either very close to the sun (0–0.15 AU), or between 0.3–0.8 AU. The minimum escape time for  $\beta = 0.3$  is about 0.66 years (7.9 months) and is found at a switching radius of about 0.53 AU. The long escape times occur when the orbit is stranded in a large elliptic orbit. For these orbits, thrust is available only for brief periods around periapsis, and the total escape time increases.

When  $\beta$  is increased to 0.4, the correlation between switching distance and escape time is very different. For  $\beta$  values of 0.4 and 0.5, the longer escape times disappear. In Fig. 3 we see that the escape time for  $\beta = 0.4$  remains almost constant between switching distances of 0.1 to 0.9 AU. So whether the control law is switched very early in the trajectory or after the solar sail has come close to the sun does not affect the escape time significantly. The minimum

escape time found for  $\beta = 0.4$  is about 0.60 years (7.2 months) and is found at a switching distance of 0.68 AU. For  $\beta = 0.5$ , we see from Fig. 3 that the time to escape is around 0.6 years (6.9 months) for all of the switching distances between 0 and 1 AU. The minimum escape time of approximately 0.58 years is found at a switching distance of 0.84 AU. In such cases where the escape times are relatively constant, it is most beneficial to switch the control close to 1 AU as this will be the least costly in terms of thermal constraints on the sail. We should note that this strategy is not equivalent to beginning from an initially circular orbit and applying the maximizing control. When the minimizing control is applied, the radius of the spacecraft actually increases slightly at the outset of the trajectory because of an increase in orbit eccentricity. Then, when the trajectory crosses 1 AU the eccentricity of the orbit is not equal to 0, and more rapid escape times are achieved than those of trajectories that begin in a circular orbit and maximize the energy increase.

**Table 1 Time to reach 100 AU (comparison with Sauer)**

$\beta$	Closest distance from sun, AU	Time to reach 100 AU, years	
		Sauer <sup>a</sup>	Our current work
0.3	0.15	10	27.88 <sup>b</sup>
0.3	0.2	11	16.79 <sup>b</sup>
0.3	0.3	13	15.02
0.3	0.4	16	17.53
0.4	0.1	6.5	7.09
0.4	0.15	7.5	7.72
0.4	0.2	9	8.64
0.4	0.3	11	10.66
0.4	0.4	13	12.8
0.5	0.1	5.5	5.19
0.5	0.15	6.5	6.24
0.5	0.2	7.5	7.21
0.5	0.3	9.5	9.02
0.5	0.4	11.5	10.77
0.59	0.1	5.0	4.63
0.59	0.15	6	5.61
0.59	0.2	7	6.50
0.59	0.3	8.5	8.11
0.59	0.4	10.5	9.65
0.79	0.1	4.0	4.00
0.79	0.15	5.0	4.83
0.79	0.2	6	5.57

<sup>a</sup>These times were estimated from Fig. 8 in Ref. 3 using characteristic accelerations that correspond with  $\beta$ .

<sup>b</sup>Corresponds to trajectories that are stranded in large elliptical orbits.

## V. Comparison with Sauer

We have compared our results with Sauer's time-optimal solar-sail trajectories to reach a particular distance.<sup>3</sup> We ran our simulations beyond escape and compared the time it took for our trajectories to reach 100 AU with those of Sauer. The results of this comparison can be found in Table 1. Sauer's globally optimized trajectories are found from satisfying the necessary conditions for optimality, whereas our trajectories follow an explicit guidance law. Surprisingly, this difference in approach has a relatively small effect on flight times in most cases. Although our locally optimal energy control law was not designed to minimize time to reach 100 AU, our flight times compare favorably with Sauer's optimized results. We note from Table 1 that for  $\beta > 0.3$  the flight times of our trajectories get close to Sauer's and even surpass them, reaching 100 AU in less time. (This might be caused by having to interpolate Sauer's time-of-flight data from a plot.) This indicates that our control methodology is in some sense near optimal for some situations. Differences between our results arise when the trajectory following our law fails to achieve escape before reaching a highly elliptical orbit.

## VI. Conclusions

This study explores the use of simple guidance laws that minimize or maximize orbit energy along a solar-sail trajectory to achieve escape conditions. We have established that maximizing the change in orbit energy at every instant along the trajectory does not necessarily minimize the time to escape. We found in general that first maximally decreasing energy and then maximally increasing energy leads to shorter escape times than escape trajectories that only maximally increase energy. These trajectories not only achieved escape in shorter time spans, but they also achieved escape using smaller values of  $\beta$  as compared with initially circular and elliptic trajectories. Using these controls, it is feasible to launch relatively poor performance solar sails ( $\beta = 0.3$ ) into escape trajectories from the sun in less than one year. For high-performance sails ( $\beta \geq 0.4$ ), the time to escape is insensitive to the energy minimizing/maximizing control strategy. Unlike most other works, we have focused on finding a general strategy for solar escape instead of designing trajectories for specific missions. Future research can begin with these simple controls to find generally applicable optimization strategies and can consider controls that maximize the final escape energy of the sail.

## References

- <sup>1</sup>Van der Ha, J. C., and Modi, V. J., "On the Maximization of Orbital Momentum and Energy Using Solar Radiation Pressure," *Journal of the Astronautical Sciences*, Vol. 27, No. 1, 1979, pp. 63–84.
- <sup>2</sup>Leipold, M., and Wagner, O., "Solar Photonic Assist Trajectory Design for Solar Sail Missions to the Outer Solar System and Beyond," *Advances in the Astronautical Sciences*, Vol. 100, No. 2, 1998, pp. 1035–1045.
- <sup>3</sup>Sauer, Carl G., Jr., "Solar Sail Trajectories for Solar Polar and Interstellar Probe Missions," *Advances in the Astronautical Sciences*, Vol. 103, Pt. 1, 2000, pp. 547–562.
- <sup>4</sup>McInnes, Colin R., *Solar Sailing Technology, Dynamics, and Mission Applications*, Praxis Publishing, Ltd., Chichester, England, U.K., 1999, pp. 38–40, 112–169.

D. Spencer  
Associate Editor

# Simulation of Wind-Profile Perturbations for Launch-Vehicle Design

S. I. Adelfang\*  
Computer Sciences Corporation,  
Huntsville, Alabama 35815

## Nomenclature

- $A_j, B_j$  = components of  $F_j$   
 $b$  = parameter for biasing an empirical gamma distribution, m/s  
 $c$  = parameter in empirical model for mean normalized power spectrum density  
 $E$  = variance coefficient of power-spectrum-density model,  $m^2/s^2$   
 $F_j$  = Fourier series,  $\sqrt{[(m^2/s^2)/(m/s)]}$   
 $n$  = wave number, 1/m  
 $r1_j, r2_j$  = random number sequences that are tangents of  $j$  uniformly distributed random phase angles in the interval from  $-\pi/2$  to  $+\pi/2$   
 $u$  and  $v$  = east–west and north–south wind components, respectively, m/s; sign convention eastward and northward wind positive  
 $z$  = altitude, km  
 $\beta$  = parameter of a gamma distribution, s/m  
 $\gamma$  = parameter of a gamma distribution  
 $\sigma$  = standard deviation of high-pass filtered wind profile, m/s

## Introduction

IDEALLY, a statistically representative sample of measured high-resolution wind profiles with wavelengths as small as tens of meters is required in design studies to establish aerodynamic load indicator dispersions and vehicle control system capability.<sup>1–3</sup> At most potential launch sites, high-resolution wind profiles might not exist. Representative samples of relatively low-resolution Rawinsonde

Presented as Paper 2003-0896 at the 41st Aerospace Sciences Meeting, Reno, NV, 9–12 January 2003; received 20 June 2003; revision received 6 April 2004; accepted for publication 6 April 2004. Copyright © 2004 by the American Institute of Aeronautics and Astronautics, Inc. The U.S. Government has a royalty-free license to exercise all rights under the copyright claimed herein for Governmental purposes. All other rights are reserved by the copyright owner. Copies of this paper may be made for personal or internal use, on condition that the copier pay the \$10.00 per-copy fee to the Copyright Clearance Center, Inc., 222 Rosewood Drive, Danvers, MA 01923; include the code 0022-4650/04 \$10.00 in correspondence with the CCC.

\*Senior Computer Engineer; currently Senior Principal Scientist, Engineering/Science, Morgan Research Corporation, Huntsville, AL 35805-1948; stan.adelfang@msfc.nasa.gov. Member AIAA.